

Search for TeV γ -ray emission from blazar 1ES1218+304 with TACTIC telescope during March-April 2013

K K Singh^a, K K Yadav^a, A K Tickoo^a, R C Rannot^a, P Chandra^a, N K Agarwal^a,
K K Gaur^a, A Goyal^a, H C Goyal^a, N Kumar^a, P Marandi^a, M Kothari^a, H Bhatt^a,
K Chanchalani^a, N Chouhan^a, V K Dhar^a, B Ghosal^a, S R Kaul^a, M K Koul^a, R
Koul^a, K Venugopal^a, C K Bhat^a, C Borwankar^a, J Bhagwan^b, A C Gupta^b

^a*Astrophysical Sciences Division, Bhabha Atomic Research Centre,
Mumbai- 400 085, India.*

^b*Aryabhata Research Institute of Observational Sciences,
Nainital- 263129, India.*

Abstract

In this paper, we present results of TeV γ -ray observations of the high synchrotron peaked BL Lac object 1ES 1218+304 ($z=0.182$) with the *TACTIC* (TeV Atmospheric Cherenkov Telescope with Imaging Camera). The observations are primarily motivated by the unusually hard GeV-TeV spectrum of the source despite its relatively large redshift. The source is observed in the TeV energy range with the *TACTIC* from March 1, 2013 to April 15, 2013 (MJD 56352–56397) for a total observation time of 39.62 h and no evidence of TeV γ -ray activity is found from the source. The corresponding 99% confidence level upper limit on the integral flux above a threshold energy of 1.1 TeV is estimated to be 3.41×10^{-12} photons $\text{cm}^{-2} \text{s}^{-1}$ (i.e. $< 23\%$ Crab Nebula flux) assuming a power law differential

Email address: kksastro@barc.gov.in (K K Singh)

energy spectrum with photon index 3.0, as previously observed by the *MAGIC* and *VERITAS* telescopes. For the study of multi-wavelength emission from the source, we use nearly simultaneous optical, UV and X-ray data collected by the UVOT and XRT instruments on board the *Swift* satellite and high energy γ -ray data collected by the Large Area Telescope on board the *Fermi* satellite. We also use radio data at 15 GHz from OVRO 40 m telescope in the same period. No significant increase of activity is detected from radio to TeV γ -rays from 1ES1218+304 during the period from March 1, 2013 to April 15, 2013.

Keywords: Blazars: 1ES 1218+304, Cherenkov Imaging telescope: Very high energy gamma-rays, Multi-wavelength observations.

1. Introduction

Blazars are observed to emit highly variable non-thermal radiation spanning the entire electromagnetic spectrum. The Spectral Energy Distribution (SED) of blazars is assumed to be dominated by emission from a relativistic jet pointing close to our line of sight. The jets in blazars consist of ultra-relativistic particles embedded in a magnetic field, with the entire plasma flowing outward from the central region with relativistic speed. The characteristic SED of blazars shows two broad non-thermal well defined continuum peaks. The first hump peaks somewhere between the infrared (IR) and X-ray bands, whereas the second hump exhibits a maximum at γ -ray energies. The origin of low energy peak is attributed to the synchrotron emission of relativistic electrons in the magnetic field of the jet. In leptonic models [1, 2, 3, 4], the γ -ray emission in High Energy (HE:

$E > 100$ MeV) and Very High Energy (VHE: $E > 100$ GeV) regimes is attributed to the inverse Compton (IC) scattering of low energy photons by the same electron population producing the synchrotron radiation (SSC: Synchrotron Self Compton) or with the possible contribution from external photons (EC: External Compton). In hadronic models [5, 6, 7, 8], both electrons and protons are accelerated to ultra-relativistic energies, with protons exceeding the threshold for photo-pion production on the soft photon field in the jet. In these models, the HE and VHE γ -ray emissions are dominated by proton synchrotron emission, neutral pion decay photons, synchrotron and Compton emission from secondary decay products of charged pions.

Blazars are broadly classified in two groups namely BL Lacertae objects (BL Lacs) and Flat Spectrum Radio Quasars (FSRQs) [9]. BL Lacs are characterized by the weak or absence of thermal features like broad emission lines in their optical spectra. On the other hand, FSRQs exhibit luminous broad emission lines in their optical spectra. The peak frequency of the synchrotron component in the SED of blazars is usually used to subdivide them in 3-classes: low-synchrotron peaked (LSP: $\nu_{peak} < 10^{14}$ Hz), intermediate-synchrotron peaked (ISP: 10^{14} Hz $< \nu_{peak} < 10^{15}$ Hz) and high-synchrotron peaked (HSP: $\nu_{peak} > 10^{15}$ Hz) blazars [10]. BL Lacs are assumed to be good VHE candidates for ground based TeV telescopes because their IC peak is in the TeV regime. To date, BL Lacs observed at VHE energies are predominantly high frequency peaked objects, which have been predicted as possible TeV candidate blazars [11].

Blazars often show violent flux variability from radio to VHE γ -rays at dif-

ferent time scales which may or may not be correlated. Therefore, simultaneous multi-wavelength (MWL) observations are important to understand the underlying physics of blazars. Furthermore, VHE observations of blazars at cosmological distances would help in constraining the intensity and spectrum of Extragalactic Background Light (EBL), which is a very important physical quantity to understand the structure and star formation history [12]. Thus, besides their importance for study of emission mechanisms and relativistic jet dynamics, growing interest for blazar study is also motivated by the use of VHE spectra as a probe for EBL [13].

1ES 1218+304 (RA: $12^h 21^m 23.5^s$, Dec: $30^\circ 10' 43.2''$) is an HSP BL Lac object located at a redshift $z = 0.182$ [14]. The source was discovered as a candidate BL Lac object on the basis of its X-ray emission and was identified as X-ray source 2A 1219+30.5 [15, 16]. Being an X-ray bright source, it was predicted to be a TeV candidate blazar from the position of the synchrotron peak in its SED [11].

The *HEGRA* (High Energy Gamma Ray Astronomy) collaboration observed 1ES 1218+304 during 1996-2002 for 3.9 h and reported an upper limit of 12% of Crab nebula flux above 750 GeV [17]. The VHE emission from 1ES 1218+304 was first detected by the *MAGIC* (Major Atmospheric Gamma ray Imaging Cherenkov) telescope in 2005 above 120 GeV [18]. The differential energy spectrum ($d\Phi/dE = f_0 E^{-\Gamma}$), with power law index (Γ) of 3.0 ± 0.4 , was also reported by the *MAGIC* group. In May 2006, 1ES 1218+304 was the target of *HESS* (High Energy Stereoscopic System) observation campaign and these observations did not yield any statistically significant signal from the source [19]. The correspond-

ing 99.9% Confidence Level (CL) limit on integral flux above 1 TeV was reported to be 17% of the *HESS* Crab Nebula flux. The *STACEE* (Solar Tower Atmospheric Cherenkov Effect Experiment) detector monitored 1ES 1218+304 during 2006-2007 above 160 GeV but did not detect any significant γ -ray emission from the source [20]. In 2007, *VERITAS* (Very Energetic Radiation Imaging Telescope Array System) telescope observed VHE emission above 160 GeV from the source at a persistent level of 6% of the Crab Nebula flux [21]. The differential energy spectrum of the source was found to be compatible with a power law of index 3.08 ± 0.34 . Using the lower limit EBL from galaxy counts [22, 23], the intrinsic power law index was found to be 2.32 ± 0.37 . During the December 2008 - May 2009 monitoring campaign of 1ES 1218+304, *VERITAS* telescope revealed a prominent flaring activity from the source at 20% of the Crab Nebula flux above 200 GeV [24]. The time averaged differential energy spectrum, in the energy range 0.2-1.8 TeV, was found to be a power law with index of 3.07 ± 0.09 . This flaring activity was characterized by a variability time scale of days. The corrected spectrum after accounting for absorption due to EBL suggests a very hard intrinsic source spectrum with index $\leq 1.28 \pm 0.28$ [25] in VHE regime based on lower limit EBL model [26].

Fermi-LAT (Large Area Telescope) also detected significant emission from 1ES 1218+304 during its first two years of operation [27]. The *Fermi*-LAT spectrum of the source is described by a power law with index 1.71 ± 0.07 , making it one of the hardest spectrum sources in MeV-GeV range. Due to relatively large redshift of the source, we expect a significant attenuation of TeV photons

above 1 TeV due to EBL absorption. This makes the source a good candidate for probing EBL using TeV observations. It is because of these characteristics of the source we were motivated to observe the source with *TACTIC* (TeV Atmospheric Cherenkov Telescope with Imaging Camera) in the TeV energy region.

The paper is organized as follows. Section 2 gives a brief description of the *TACTIC* telescope and in Section 3 we present details of observation and data analysis. In Section 4 we present the MWL data analysis of the source from radio to HE. In Section 5 we discuss the results and the conclusions are presented in Section 6.

2. TACTIC Telescope

The *TACTIC* γ -ray telescope is located at Mount Abu (1300 m asl, 24.6°N, 72.7°E), India [28]. The telescope is equipped with a F/1-type tessellated light collector of approximately 9.5 m^2 area consisting of 34 front-face aluminium coated, spherical glass mirror facets of 60 cm diameter. The point-spread function has a full width at half maxima (FWHM) of 0.185° ($\equiv 12.5\text{mm}$) and $D_{90} \sim 0.34^\circ$ ($\equiv 22.8\text{mm}$). Here, D_{90} is defined as the diameter of a circle, concentric with the centroid of the image, within which 90% of reflected rays lie. The telescope deploys a 349-pixel imaging camera, with a uniform pixel resolution of 0.31° and a $5.9^\circ \times 5.9^\circ$ field-of-view, to record atmospheric Cherenkov events produced by an incoming cosmic-ray particle or a γ -ray photon. Data used in this work have been collected with inner 225 pixels where the innermost 121 pixels (11×11 matrix) are used for generating the event trigger. The trigger scheme is based on a Near-

est Neighbour Non-collinear Triplets trigger criterion. Apart from generating the prompt trigger with a coincidence gate width of $\approx 18\text{ns}$, the trigger generator has a provision for producing a chance coincidence output based on $^{12}C_2$ combinations from various groups of closely spaced 12 channels. The data acquisition and control system of the telescope is designed around a network of PCs running the QNX (version 4.25) real-time operating system. The triggered events are digitized by CAMAC based 12-bit charge to digital converters (CDC), which have a full scale range of 600 pC. The relative gain of the photomultiplier tubes is monitored regularly once in 15 minutes by flashing a blue LED, placed at a distance of about 1.5m from the camera. Other details regarding hardware and software features of the data acquisition and control system of the telescope are discussed in [29].

Major upgrade, involving replacement of signal and high voltage cables and installation of new Compound Parabolic Concentrators (CPC) was taken up in November-December 2011 for improving the sensitivity of the telescope. While detailed simulation and experimental results on the Crab Nebula, after upgrade will be presented elsewhere, we present here only a brief summary of the upgrade work. New CPCs with square entry and circular exit aperture were installed on the *TACTIC* imaging camera in order to increase its photon collection efficiency. The collection efficiency of the new CPCs was measured to be about 80% in the wavelength range 400–550 nm. Apart from removing the dead space in between the photomultipliers substantially, the new CPCs has also helped us to improve the gamma/hadron segregation capability of the telescope. In addition, the trigger criteria was also modified by including more nearest neighbor collinear triplet

combinations. A dedicated CCD camera was also installed for conducting detailed point run calibrations and data collected were successfully used for determining the position of the source in the image plane with an accuracy better than ± 3 arc min. The point run calibration data (i.e. position of the star image in the camera) were also incorporated in the analysis software so that appropriate corrections can be applied in an off line manner while calculating source position dependent image parameters. The analysis procedure was improved by using the Asymmetry parameter so that additional hadronic background can be further removed by identifying the “head/tail” feature of Cherenkov images. It is worth mentioning here that the γ -ray images have their head closer to the assumed source position in the imaging camera and thus can be selected preferentially by imposing Asymmetry >0 cut.

The upgrade of the telescope has led to an increase in the prompt coincidence rate from 2.33 Hz to 4.70 Hz close to the zenith. Furthermore, as a result of the upgrade the γ -ray rate from the Crab Nebula has also increased from 9.13 h^{-1} to 15.30 h^{-1} and this translates to the reduction in the telescope threshold energy from 1.2 TeV to 0.87 TeV.

3. TACTIC Observations and Results

The blazar 1ES 1218+304 was monitored with the *TACTIC* from March 1, 2013 to April 15, 2013 (MJD 56352–56397) at zenith angles between 6° and 45° . All the data were collected in tracking mode, during which the telescope continuously monitored the source. This mode of observation maximizes the source

observation time and increases the possibility of detecting flaring activity from the source. About 54 h of data were collected during 18 nights of observations as per the details summarized in Table 1.

Table 1: Summary of *TACTIC* observations of 1ES 1218+304

Month	Observation dates	Observation Time (h)	Selected data (h)
March 2013	3,4,8,9,10,12,13,14,17,18,19	26.00	16.79
April 2013	6,7,9,10,11,12,13	28.00	22.83
Total	18 Nights	54.00	39.62

3.1. *TACTIC* Data Analysis

Apart from excluding the observations during bad atmospheric conditions, several standard data quality tests have been applied to the raw data for selecting clean data for further analysis. The data quality checks include the following: compatibility of the prompt coincidence rates with the expected zenith angle behavior, Poission distribution for arrival times of prompt events and steady behavior of chance coincidence rates with time. After applying the above data quality checks the final data sample reduces to ~ 39.62 h. For gamma/hadron separation we have followed the standard Hillas parameter analysis [30] where each Cherenkov image is characterized by its moments. In this procedure each Cherenkov image is characterized by various image parameters like *length* (L), *width* (W), *distance* (D), *alpha* (α), *size* (S), *frac2* (F2) and *asymmetry* (ASYM). This technique was later refined to Dynamic Supercuts procedure where *S* dependent shape parameters of the image as well as its orientation were used for

segregating the γ -rays from the background cosmic-rays [31, 32]. The γ -ray selection criteria used in the present work are given in Table 2. These cuts have been optimized using 25 h of actual observation data on the Crab Nebula during November 2012. When applied to the remaining data on the Crab Nebula, the above cuts yield consistent detection of a γ -ray signal at a sensitivity level of $N_\sigma \sim 1.40 \sqrt{T}$ (where T is the observation time in hours).

Table 2: Dynamic Supercuts selection criterion used for analyzing the *TACTIC* data.

Parameters	Cuts Value
L	$0.11^\circ \leq L \leq (0.1000 + 0.0520 \times \ln S)^\circ$
W	$0.06^\circ \leq W \leq (0.0850 + 0.0160 \times \ln S)^\circ$
D	$0.50^\circ \leq D \leq (1.27 \times \cos^{0.95}\theta)^\circ$ (θ =zenith angle)
S	≥ 310 dc (digital counts)
α	$\alpha \leq 18^\circ$
F2	≥ 0.35
L/W	≥ 1.55
ASYM	≥ 0.0

A well established procedure to extract the γ -ray signal from the cosmic ray background is to plot the frequency distribution of α parameter (defined as the angle between the major axis of the image and the line between the image centroid and camera center) of shape (L,W) and D selected events. This distribution is expected to be flat for the isotropic background of cosmic events. For γ -rays, coming from a point source, the distribution is expected to show a peak at smaller α values. Defining $\alpha \leq 18^\circ$ as the γ -ray domain and $27^\circ \leq \alpha \leq 81^\circ$ as the background region, the number of γ -ray events is then calculated by subtracting the expected number of background events (calculated on the basis of background

region) from the γ -ray domain events. The statistical significance of γ -ray like events is calculated using the methodology proposed by Li and Ma [33].

In order to validate the proper functioning of the telescope and the data analysis methodology, we are collecting data on the Crab Nebula regularly. Although, during the observing season 2012-2013, the Crab Nebula was observed with *TACTIC* right from November 2012 onwards, we present here, as a representative example, the results of our observations for approximately 11.33 h only, which were carried out from March 1, 2013 to March 13, 2013. The main purpose of doing this is to compare the results of the Crab Nebula observations with that of 1ES1218+304. There is an overlap of 6 nights when both the Crab Nubula and 1ES1218+304 have been observed one after the other. Figure 1(a) gives the α -distribution when the data collected on the Crab Nebula for 11.33 h is analyzed. The events selected after using the Dynamic Supercuts procedure yield an excess of 169 ± 32 γ -ray like events with a statistical significance of 5.47σ . The corresponding γ -ray rate turns out to be $(14.91 \pm 2.82) \text{h}^{-1}$. Since the average zenith of 28° for 11.33 h data on the Crab Nebula is close to the average zenith of 21° for 39.62 h data on 1ES1218+304, one can express the γ -ray rate observed from 1ES1218+304 in Crab Unit (CU: $1 \text{ CU} \equiv 14.91 \pm 2.82 \text{ h}^{-1}$). Figure 1(b) gives the α -distribution for the data collected on 1ES 1218+304 for 39.62 h. The analysis of the data yields an excess of 2 ± 56 γ -ray events with a statistical significance of 0.04σ , which suggests that there is no evidence for a γ -ray signal from the source during the period of our observations. The source is thus possibly in a low state which is below the sensitivity level of the *TACTIC*. The upper limit estimation on the

integral VHE γ -ray flux from the source is described below.

3.2. Upper Limit Calculation for TACTIC

Using the probability density function of the number of excess events we have determined the upper limit on the excess events (N_{UL}) by using the methodology proposed by Helene [34] and the method involves solving the following equation for N_{UL} ,

$$\beta I\left(\frac{-N_{exc}}{\sigma_{exc}}\right) = I\left(\frac{N_{UL} - N_{exc}}{\sigma_{exc}}\right) \quad (1)$$

where $(1-\beta) \times 100\%$ is the confidence level, N_{exc} is number of excess events with σ_{exc} as its standard deviation. The function $I(x)$ is given by

$$I(x) = \frac{1}{\sqrt{2\pi}} \int_x^\infty e^{-t^2/2} dt = \frac{1}{2} \operatorname{erfc}\left(\frac{x}{\sqrt{2}}\right) \quad (2)$$

Where $\operatorname{erfc}(x)$ is the complementary error function. On solving equation 1 with $N_{exc} = 2$, $\sigma_{exc} = 56$ (refer α -plot shown in Figure 1(b)) and $\beta = 0.01$, we get $N_{UL} \approx 146$ as 99% confidence level upper limit on the excess events from the source. Knowing that the γ -ray rate of $(14.91 \pm 2.82) \text{h}^{-1}$ corresponds to 1 CU, the resulting 99% limit on the rate of excess events from 1ES1218+304 translates to 3.68h^{-1} (i.e $146/39.62 \text{h}$ or 0.25 CU). Alternatively, on dividing the upper limit on the excess events by the product of effective collection area $\sim 3.0 \times 10^8 \text{ cm}^2$ (obtained after applying the Dynamic Supercuts) and observation time $\sim 39.62 \text{ h}$, we find the 99% upper limit on the integral flux to be $3.41 \times 10^{-12} \text{ photons cm}^{-2} \text{ s}^{-1}$ above threshold energy of 1.1 TeV. The values of effective collection

area and threshold energy used above correspond to zenith angle of 25° . If we assume a source spectrum similar to that of the Crab Nebula (i.e $d\Phi/dE = 2.79 \times 10^{-11} E^{-2.59} \text{ cm}^{-2} \text{ s}^{-1} \text{ TeV}^{-1}$; as measured by the *HEGRA* group [35]) and also found to match very well with the spectrum obtained from the *TACTIC* [28], the above 99% limit translates to an integral flux upper limit of 0.26 CU. Referring back to the upper limit, if we assume a steeper spectrum (i.e $d\Phi/dE \propto E^{-3.0}$) for 1ES1218+304, similar to the one observed by *MAGIC* and *VERITAS* telescopes [18, 21], the above upper limit on the integral flux corresponds to about 0.23 CU above a threshold energy of 1.1 TeV. The differential flux upper limit at 99% confidence level is found to be $6.2 \times 10^{-12} \text{ photons cm}^{-2} \text{ s}^{-1} \text{ TeV}^{-1}$.

4. Analysis of multi-wavelength data

The MWL data for 1ES 1218+304 were collected in optical and UV by *Swift*-UVOT, in X-rays by *Swift*-XRT, and in HE γ -rays by *Fermi*-LAT during March 1, 2013 to April 15, 2013 (MJD 56352–56397). The details of observation and data reduction for these instruments are described below.

4.1. *Fermi*-LAT data

The *Fermi*-LAT is a pair conversion γ -ray telescope sensitive to photon energy in the MeV-GeV regime [36]. The instrument has been designed to measure the directions, energies and arrival times of incident photons in the energy range 20 MeV to $> 300 \text{ GeV}$ while rejecting the background from cosmic rays. In its nominal scanning mode, it surveys the whole sky every 3 h with a large field

of view of about 2.4 steradian. The *Fermi*-LAT data for 1ES 1218+304 were retrieved from the publicly available NASA data base¹ during the period March 1, 2013 to April 15, 2013 (MJD 56352–56397). We selected the good quality events from the “source class” over the energy range 100 MeV–100 GeV and the events were extracted from a circular region of interest (ROI) with radius 15° centered at the source position (RA= $12^h21^m23.5^s$, Dec= $30^\circ10'43.2''$). In addition, we excluded the events observed with zenith angles $> 100^\circ$ to limit contamination from Earth limb γ -rays, and events detected while the spacecraft rocking angle was $> 52^\circ$ to avoid time intervals during which the bright limb of the Earth entered the LAT field of view.

The data obtained in this manner were analyzed using the standard *Fermi* Science-Tools software package (version v9r27p1). We used P7_SOURCE_V6 instrument response function with the galactic and isotropic diffuse emission models gal_2yearp7v6_v0.fits and iso_p7v6source.txt. All the point sources from *Fermi*-LAT second source catalog (2FGL) [27] within 20° of 1ES 1218+304, including the source of interest itself were considered in source model file. Sources within the ROI were fitted with power law models with the normalization and spectral index as free parameters, while those beyond ROI had their model parameters frozen to those as reported in second source catalog [27]. An unbinned likelihood spectral analysis was performed to produce the light curve with the standard analysis tool *gtlike* implemented in Science-Tools software package. Since the source

¹<http://fermi.gsfc.nasa.gov/ssc/data/access>

is not always detected at high statistical significance, we have produced the five day binned light curve with minimum statistical significance accepted for each time bin as $TS \geq 4$, where TS is the test statistic defined as twice the difference of the log(likelihood) with and without the source respectively [37]. The time averaged spectrum of the source was obtained by fitting a power law model with the normalization as free parameter and spectral index set to the value obtained by integrating the data over entire period of observation in the energy range 100 MeV-100 GeV. The details of the source spectrum obtained in the present work from *Fermi*-LAT observations are described in Section 5.2.

4.2. *Swift*-XRT & *UVOT* data

During March 1, 2013 to April 15, 2013 (MJD 56352–56397) only six days of observations are available from *Swift* with XRT (X-Ray Telescope), covering the 0.3-10 keV energy band [38], and UVOT (UV/Optical Telescope), covering 180-600 nm wavelength range [39].

Swift-XRT data were reduced following the standard procedure² using *FTOOLS*. The data were collected in window timing (WT) mode for all the observations. The task XSELECT (ver V2.4b) within the HEASOFT package (v6.13) with recent calibration files (ver. 20120209) was used to analyse the data. The spectra and light curves of the source were extracted using a circular region with radius of 23'' around the source. The spectra and light curves of nearby background region were extracted within an annulus with inner radius of 24'' and outer radius of 45''

²<http://www.swift.ac.uk/analysis/xrt/>

around the source. The corresponding exposure maps and ancillary response files (ARFs) were generated using the tasks XRTEXPOMAP and XRTMKARF for all the observations, respectively. The spectra were binned using GRPPHA to ensure a minimum of 20 counts per bin to perform the χ^2 minimization for fitting the spectrum with model *phabs*zpowerlaw* and the fluxes were calculated using CFLUX. The best-fit parameters given in Table 3 were derived for individual observation with a neutral hydrogen column density fixed to its Galactic value $1.99 \times 10^{20} \text{ cm}^{-2}$ obtained from NASA/IPAC Extragalactic Database (NED)³. The best fit average parameters were also derived using simultaneous fitting of the spectra of six observations.

The source 1ES 1218+304 was observed with *Swift*-UVOT using all filters (V, B, U, UVW1, UVM2, UVW2) in image mode over six days during *TACTIC* observations. The image mode level II data of all the filters were used in the present analysis with latest calibration files of UVOT [40]. The data were processed with the standard procedure⁴ using UVOTMAGHIST task of HEASOFT package. The UVOT source counts were extracted from a 5'' sized circular region centered on the source position, while the background was extracted from a nearby larger, source free, circular region of 10'' radius. The observed magnitudes were converted into fluxes using conversion factors given in [41]. The observed magnitudes obtained in six filters during the period from March 1, 2013 to April 15, 2013 are reported in Table 4.

³ned.ipac.caltech.edu

⁴<http://www.swift.ac.uk/analysis/uvot/>

Table 3: Spectral analysis of *Swift*-XRT data during March 1, 2013 to April 15, 2013 using power law spectrum with neutral hydrogen density fixed at $1.99 \times 10^{20} \text{ cm}^{-2}$.

MJD	Obs-ID	Photon index	Flux ($10^{-11} \text{ erg cm}^{-2} \text{ s}^{-1}$)	$\chi^2_{red}(dof)$
56360	sw00030376021	$2.05^{+0.04}_{-0.04}$	$4.89^{+0.06}_{-0.06}$	1.23 (48)
56366	sw00030376022	$1.94^{+0.04}_{-0.04}$	$6.49^{+0.08}_{-0.09}$	0.90 (51)
56369	sw00030376023	$2.11^{+0.04}_{-0.03}$	$5.84^{+0.06}_{-0.06}$	0.80 (64)
56387	sw00030376024	$2.23^{+0.05}_{-0.05}$	$4.03^{+0.06}_{-0.06}$	0.93 (43)
56390	sw00030376025	$2.13^{+0.05}_{-0.04}$	$4.42^{+0.06}_{-0.06}$	1.43 (46)
56396	sw00030376026	$2.23^{+0.04}_{-0.04}$	$4.31^{+0.05}_{-0.05}$	1.38 (58)

Table 4: Summary of *Swift*-UVOT observed magnitudes during March 1, 2013 to April 15, 2013 in six filters.

MJD	V	B	U	W1	M2	W2
56360	16.15 ± 0.08	16.78 ± 0.06	15.86 ± 0.05	15.85 ± 0.05	15.59 ± 0.04	15.83 ± 0.03
56366	16.43 ± 0.01	16.98 ± 0.07	15.96 ± 0.05	16.06 ± 0.05	16.30 ± 0.07	16.24 ± 0.04
56369	16.27 ± 0.08	16.87 ± 0.06	16.01 ± 0.05	15.91 ± 0.05	15.79 ± 0.05	15.80 ± 0.03
56387	16.30 ± 0.08	16.76 ± 0.06	15.95 ± 0.05	15.85 ± 0.05	15.79 ± 0.05	15.87 ± 0.04
56390	16.17 ± 0.08	16.86 ± 0.06	16.10 ± 0.05	15.89 ± 0.05	15.76 ± 0.05	15.84 ± 0.04
56396	16.21 ± 0.07	16.79 ± 0.05	15.82 ± 0.04	15.76 ± 0.04	15.72 ± 0.04	15.88 ± 0.03

4.3. *OVRO data*

The *OVRO* (Owens Valley Radio Observatory) is a fast cadence 15 GHz radio telescope with diameter of 40 m [42]. The telescope is a f/0.4 type parabolic reflector on an alt-azm mounting system and is equipped with dual beamed off axis optics and a cooled receiver installed at prime focus. The source 1ES 1218+304 was observed at 15 GHz using *OVRO* telescope⁵ for six days during *TACTIC* observations as part of *Fermi* MWL blazar monitoring program and data of these observations are used in the present work.

5. Results and Discussion

5.1. *Light curve analysis*

The MWL light curve of 1ES 1218+304 observed by various instruments during March 1, 2013 to April 15, 2013 (MJD 56352–56397) is shown in the Figure 2. Since no significant γ -ray emission has been detected from the source with the *TACTIC*, we have shown the 99% CL upper limit on integral flux above 1.1 TeV for *TACTIC* observations in Figure 2(a). The five-day binned light curve of the source observed with *Fermi*-LAT during the same period is presented in Figure 2(b). All the points reported in the Figure 2(b) correspond to $TS > 4$. From the figure, it is evident that there is no statistically significant variation in the γ -ray activity in the energy range 100 MeV-100 GeV during *TACTIC* observations and the average flux level during this period is found to be $(4.17 \pm 0.82) \times 10^{-8}$

⁵www.astro.caltech.edu/ovroblazars/data

photons $\text{cm}^{-2} \text{s}^{-1}$. It is important to mention here that the source has been categorized as highly variable on monthly time scale in the second *Fermi* catalog [27] and thus some enhanced activity may be quite consistent with its past behavior.

Nearly simultaneous X-ray light curve observed by *Swift*-XRT for six days of monitoring of the source is depicted in Figure 2(c). From the figure, we observe that the soft X-ray emission from the source is consistent with the average flux level $(5.01 \pm 0.34) \times 10^{-11} \text{ erg cm}^{-2} \text{s}^{-1}$, except for some enhanced activity on March 15, 2013 (MJD 56366). During the enhanced activity on March 15 in X-rays, the HE activity is also observed to be slightly higher with respect to the average flux. We have also looked into the archival X-ray data in the energy bands 2-20 keV and 15-50 keV from *MAXI*⁶ and *Swift*-BAT⁷ instruments respectively and these data do not show any detection above 3σ . This indicates that during the period of *TACTIC* observations, the source was not active in hard X-ray regime. The simultaneous UV (W1,M2,W2 filters) and optical(V,B,U filters) light curves of the source for six days of observations are presented in Figure 2(d) and 2(e) respectively. The UVOT flux points included in the light curve have not been de-reddened. No unusual activity is observed in the source with *Swift*-UVOT instrument during the period of *TACTIC* observations. The radio observations at 15 GHz available for six days are shown in Figure 2(f). No significant variations are observed in radio emission from the source during this period.

⁶<http://maxi.riken.jp/top/index.php>

⁷<http://heasarc.nasa.gov/docs/swift/results/transients>

5.2. Spectral Analysis

The spectral energy distribution of 1ES1218+304 during March 1, 2013 to April 15, 2013 using broad band data discussed above is shown in Figure 3. For VHE γ -rays we plot the data from the observations with *MAGIC* and *VERITAS* telescopes along with the 99% confidence level upper limit on integral flux obtained from *TACTIC* in the present work. The flux points reported by *MAGIC* group are based on the observations carried out during the period January 9-15, 2005 [18]. During six days of observations, no flux variability on timescales of days was found and the time averaged spectrum was described by a power law with $\Gamma = 3.0 \pm 0.4$. The *VERITAS* flux points taken from [21] correspond to observations during January-March 2007 for a total observation time of 17.4 h. The time averaged differential spectrum was described by a power law with photon index 3.08 ± 0.34 and the integral flux above 200 GeV was 6% of the Crab Nebula flux. It is evident from the figure that the measured flux points are consistent with each other in the overlapping energy regime of the two telescopes. The VHE flux points measured with *MAGIC* and *VERITAS* telescopes as well as upper limit from *TACTIC* have been corrected for EBL absorption using the mean level density model proposed by Franceschini et al. (2008) [43].

The LAT data points have been obtained by dividing the energy range 0.1–100 GeV into four energy bands: 0.1–1 GeV, 1–10 GeV, 10–20 GeV and 20–100 GeV. The time averaged GeV spectrum measured by *Fermi*-LAT during this period is described by a power law with normalization factor $f_0 = (8.47 \pm 1.20) \times 10^{-9} \text{ cm}^{-2} \text{ s}^{-1} \text{ GeV}^{-1}$ and photon index $\Gamma = 1.78 \pm 0.06$. The HE photon index

$\Gamma=1.78\pm0.06$ obtained in the present study is consistent with the value reported from quiescent state monitoring of 1ES 1218+304 by *Fermi*-LAT [44, 45]. The photon index observed by *Fermi*-LAT during the first two years of observation of 1ES 1218+304 is 1.709 ± 0.067 [27].

The *Swift*-XRT flux points have been obtained from simultaneous fitting of the spectra of six observations in three energy bands: 0.3-1 keV, 1-2.5 keV and 2.5–6 keV using CFLUX. Beyond 6 keV, *Swift*-XRT observations are not statistically significant to perform spectral analysis. The X-ray flux points measured with XRT as shown in Figure 3 have been corrected for Galactic absorption using a neutral hydrogen column density of $1.99\times10^{20} \text{ cm}^{-2}$ obtained from NED⁸. The time averaged soft X-ray spectrum measured with XRT during *TACTIC* observations is described by a power law with photon index 2.13 ± 0.01 . The X-ray emission level of $(1.93\pm0.01)\times 10^{-11} \text{ erg cm}^{-2} \text{ s}^{-1}$ in the energy range 2-10 keV, observed in our present study is below the flux level $(2.64\pm0.02)\times 10^{-11} \text{ erg cm}^{-2} \text{ s}^{-1}$ obtained from *XMM-Newton* measurements during 2001 observations [46].

The simultaneous optical and UV emission in the wavelength range 180-600 nm as measured by *Swift*/UVOT instrument in all six filters (V,B,U,W1,M2,W2) is shown in the Figure 3. The flux densities in all filters are estimated from the dereddened magnitudes with galactic absorption $A_v = 0.056$ and $R_v = A_v/E(B - V) = 3.1$ [47], using the methodology proposed in [41]. The UVOT flux points

⁸ned.ipac.caltech.edu

have been obtained by multiplying the mean of flux densities with the bandpass (FWHM) of the corresponding filter [41]. Error in the mean density is obtained through the standard error propagation method. The radio flux point at 15 GHz obtained from OVRO telescope data archive⁹ corresponds to the mean emission level from the source during *TACTIC* observations.

The broadband data points presented in Figure 3 indicate that the SED of the source can be described by two humps: first one peaking at X-ray energies and second at GeV energies. This implies that the MWL emission from 1ES 1218+304 can be possibly compared with the predictions of SSC model for blazar emission, but detailed SED modeling of the source is beyond the scope of this work.

Tang et al. (2010) have reproduced the SED of 1ES 1218+304 with the inhomogeneous jet model and the homogeneous SSC model [48]. They emphasize that the leptonic model is very successful in explaining multi-band emissions from the source and also point out that the VHE γ -ray data from the *MAGIC* and *VERITAS* telescopes can be fitted with the strict lower-limit EBL model. Using the *Swift*, *MAGIC* and *VERITAS* telescopes data the SED of the source has been modeled in [49] by employing a time-dependent SSC code for obtaining the physical parameters of the emission region. The short-time variability of the source has also been studied by Weidinger & Spanier (2010) [50] for reproducing the light curve observed by *VERITAS* telescope. They suggest that the light curve can be reproduced by assuming a changing level of electron injection

⁹<http://www.astro.caltech.edu/ovroblazars/data/data.php>

compared to the constant state.

6. Conclusions

Our γ -ray observations of 1ES 1218+304 ($z=0.182$) with the *TACTIC* from March 1, 2013 to April 15, 2013 (MJD 56352-56397) for a total observation time of ~ 39.62 h do not show any evidence of TeV γ -ray signal from the source. The MWL data in the X-ray and HE bands, as measured by *Swift*-XRT (0.3-10 keV) and *Fermi*/LAT (0.1–100 GeV) respectively, do not reveal any unusual activity from the source. The optical and UV emissions observed with *Swift*-UVOT instrument and radio observations at 15 GHz with 40 m *OVRO* telescope during *TACTIC* observations also do not indicate any flaring activity from the source. It is important to point out here that, because of the variable nature of blazars in general, the VHE emission from 1ES1218+304 may increase significantly during future flaring episodes and may even easily exceed the limit reported in the present work. Hence the upper limit presented here only constrains the flux during our observation period. Our blazar observation program will continue to monitor this source.

Acknowledgment

We thank the anonymous reviewer for his/her suggestions which improved the quality of the paper. The authors would like to convey their gratitude to all the concerned colleagues of the Astrophysical Sciences Division for their contributions towards the instrumentation, observation and analysis aspects of the *TACTIC*

telescope. We acknowledge the useful discussions held with N.G. Bhatt on various aspects of data analysis. We acknowledge the use of public data obtained through *Fermi* Science Support Center (FSSC) provided by NASA. This work made use of data supplied by the UK *Swift* Science Data Centre at the University of Leicester. This research has made use of the NASA/IPAC Extragalactic Database (NED) which is operated by the Jet Propulsion Laboratory, California Institute of Technology, under contract with the National Aeronautics and Space Administration.

References

- [1] L. Maraschi et al. 1992, ApJ, 397, L5
- [2] C. Dermer and R. Schlickeiser, 1993, ApJ, 416, 458
- [3] M. Sikora et al., 1994, ApJ, 421, 153
- [4] M. Blazejowski et al., 2000, ApJ, 545, 107
- [5] K. Mannheim and P. L. Biermann, 1992, A&A, 253, L21
- [6] F. Aharonian et al., 2000, New Astron., 5, 377
- [7] A. Mucke and R. J. Protheroe, 2001, Astropart. Phys., 15, 121
- [8] A. Mucke et al., 2003, Astropart. Phys., 18, 593
- [9] C. Urry and P. Padovani, 1995, PASP, 107, 803

- [10] A. A. Abdo et al., 2010, ApJ, 716, 30
- [11] L. Costamante and G. Ghisellini, 2002, A&A, 384, 56
- [12] F. W. Stecker et al., 1992, ApJ, 390, L49
- [13] F. Aharonian et al., 2006, Nature, 440, 1018
- [14] N. Bade et al., 1998, A&A, 334, 459
- [15] A. S. Wilson et al., 1979, MNRAS, 187, 109
- [16] J. E. Ledden et al., 1981, ApJ, 243, 47
- [17] M. Tluczykont et al., 2003, 28th ICRC, 2547
- [18] J. Albert et al., 2006, ApJ, 642, L119
- [19] F. Aharonian et al., 2008, A&A, 478, 387
- [20] C. Mueller et al., 2011, Astropart. Phys., 34, 674
- [21] A. Acciari et al., 2009, ApJ, 695, 1370
- [22] P. Madau and L. Pozzetti, 2000, MNRAS, 312, L9
- [23] G. G. Fazio et al., 2004, ApJS, 154, 39
- [24] A. Acciari et al., 2010, ApJL, 709, L163
- [25] F. Krennrich et al., 2008, ApJ, 689, L23
- [26] L. Levenson and E. Wright, 2008, ApJ, 683, 585

- [27] P. L. Nolan et al., 2012, ApJS, 199, 31
- [28] R. Koul et al., 2007, NIM A, 578, 548
- [29] K. K.Yadav et al., 2004, NIM A, 527, 411
- [30] A. M. Hillas et al., 1985, Proc. 19th ICRC, 3, 445
- [31] A. M. Hillas et al., 1998, ApJ, 503, 744
- [32] G. Mohanty et al., 1998, ApJ, 9, 15
- [33] T. P. Li and Y. Q. Ma, 1983, ApJ, 272, 317
- [34] O. Helene, 1983, NIM A, 212, 319
- [35] F. A. Aharonian et al., 2000, ApJ, 539, 317
- [36] W. B. Atwood et al., 2009, ApJ, 697, 1071
- [37] J. R. Mattox et al., 1996, ApJ, 461, 396
- [38] D. N. Burrows et al., 2005, Space Sci. Rev. 120, 165
- [39] P. W. A. Roming et al., 2005, Space Sci. Rev. 120, 95
- [40] A. A. Breeveld et al., 2011, AIPC, 1358, 373
- [41] T. S. Poole et al., 2008, MNRAS, 383, 627
- [42] J. L. Richards et al., 2011, ApJS, 194, 29
- [43] A. Franceschini et al., 2008, A&A, 487, 837

- [44] A. A. Abdo et al., 2009, ApJ, 700, 597
- [45] A. A. Abdo et al., 2009, ApJ, 707, 1310
- [46] A. J. Blustin, M. J. Page and G. B. Rayment, 2004, A&A, 417, 61
- [47] E. F. Schlafly and D. P. Finkbeiner, 2011, ApJ, 737, 103
- [48] Y. Tang, Z. Dai and L. Zhang, 2010, RA&A 10, 415
- [49] M. Ruger et al., 2010, MNRAS, 401,973
- [50] M. Weidinger and F. Spanier, 2010, A&A, 515, A18

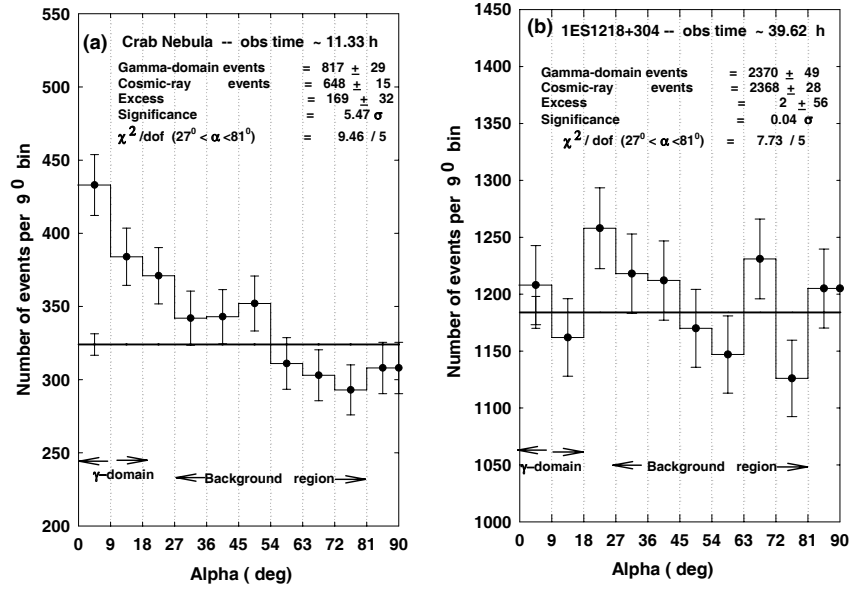


Figure 1: (a) On-source alpha plot of Crab Nebula for 11.33 h of data collected during March 1, 2013 to March 13, 2013 (b) On-source alpha plot of 1ES1218+304 for 39.62 h of data collected during March 1, 2013 to April 15, 2013 (MJD 56352–56397). The horizontal lines in these figures indicate the expected background in the γ -domain obtained by using the background region with $27^\circ \leq \alpha \leq 81^\circ$.

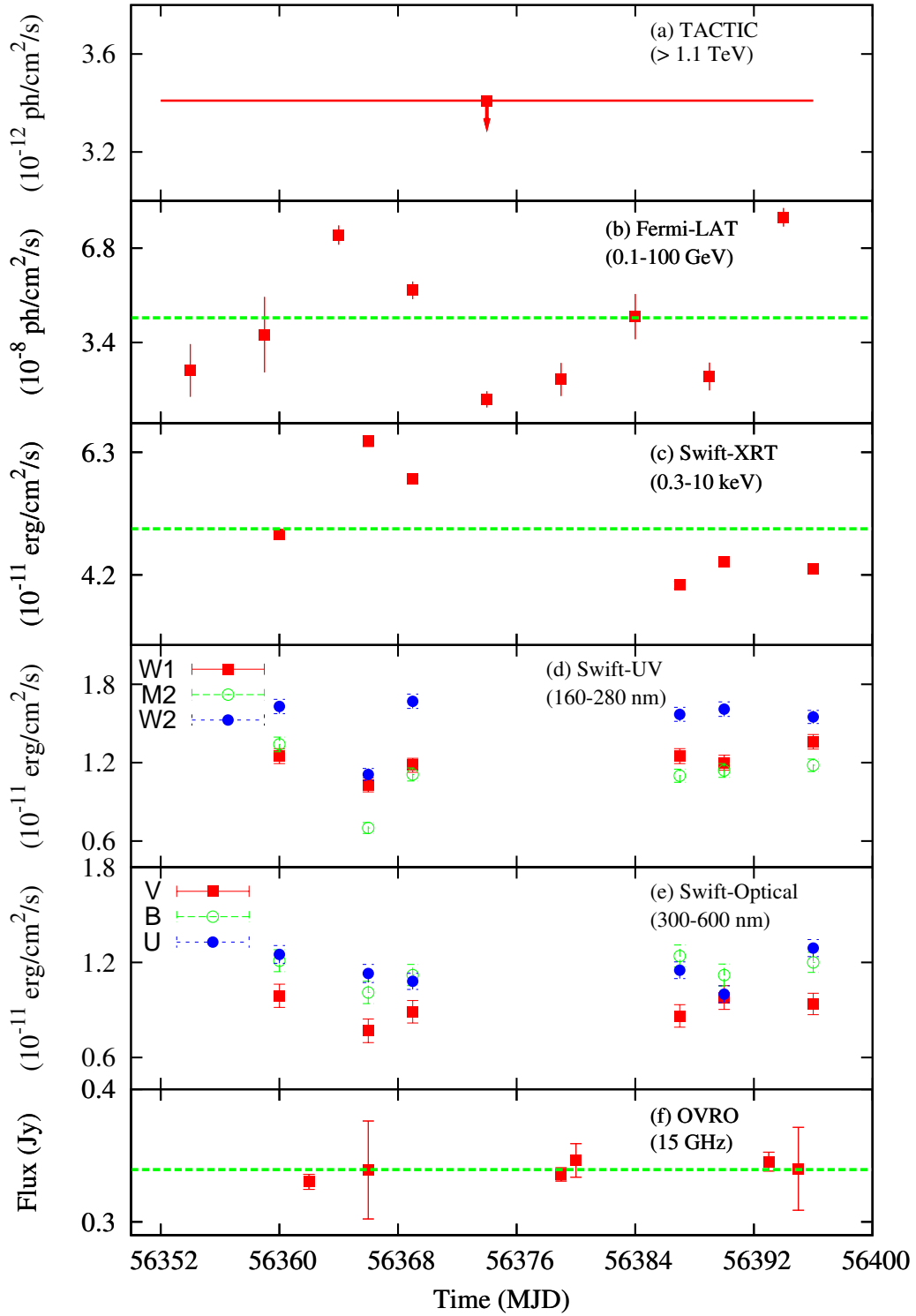


Figure 2: Multi-wavelength light curve of 1ES 2218+304 during March 1, 2013 to April 15, 2013 covering VHE γ -rays by *TACTIC*, HE γ -rays by *Fermi*-LAT, X-rays by *Swift*-XRT, UV/optical by *Swift*-UVOT instruments and radio by *OVRO* telescope. 99% confidence upper limit in VHE γ -rays by *TACTIC* is indicated as downward arrow. Each point in the 5 day binned light curve of *Fermi*-LAT in HE γ -rays corresponds to TS > 4. X-ray, UV/Optical and radio light curves represent daily flux values for 6 days of observations available during the monitoring of the source with *TACTIC*. The horizontal dotted lines (shown in (b), (c) & (f)) represent the average emission level in the respective energy bands.

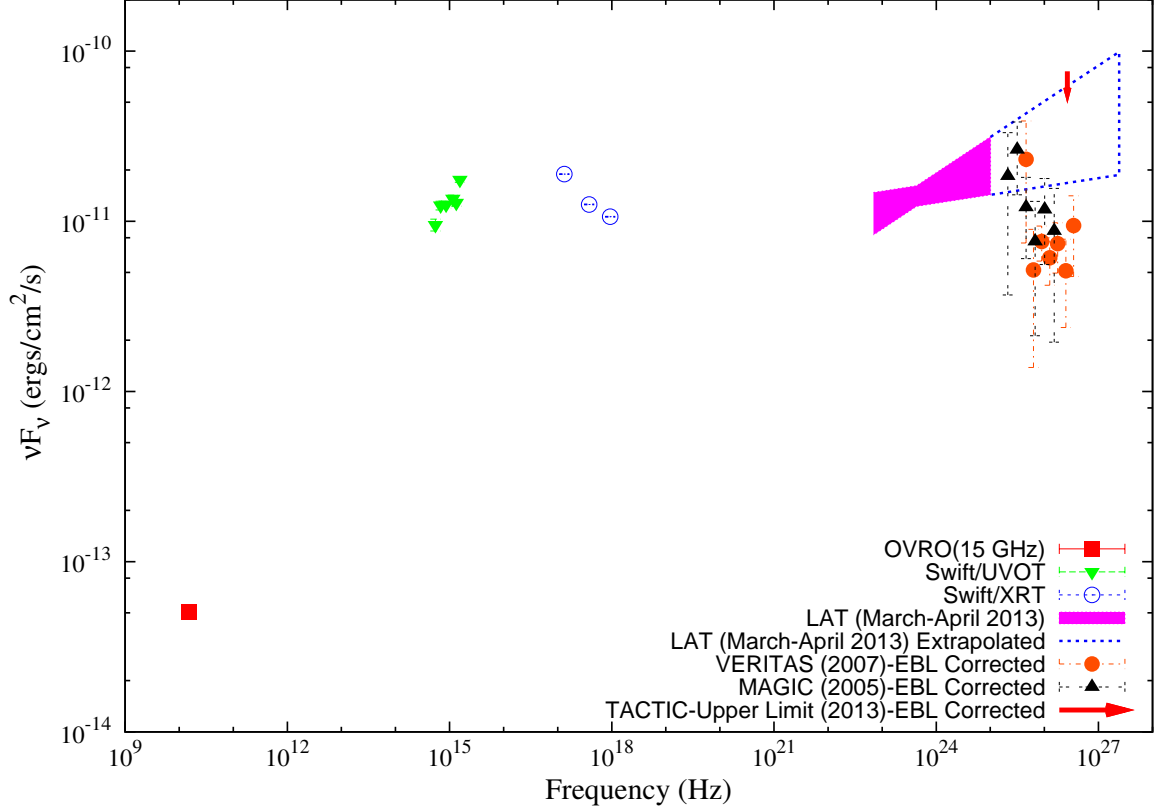


Figure 3: Multi-wavelength SED of 1ES1218+304 measured during March 1, 2013 to April 15, 2013. VHE points correspond to the fluxes measured by: *MAGIC* [18], *VERITAS* [21] telescopes along with *TACTIC* 99% flux upper limit at ~ 1.1 TeV (present work). All the VHE flux points have been corrected for EBL absorption using Franceschini et al. (2008) model [43]. *Fermi*-LAT spectrum measured during March-April 2013 is shown as butterfly (filled curve) and same has been extrapolated in the *TACTIC* energy range 0.87–10 TeV (dotted lines). *Swift*-XRT points are time averaged fluxes for six days of observations. *Swift*-UVOT points correspond to time averaged fluxes measured in all filters (V,B,U,W1,M2,W2). The time averaged radio flux at 15 GHz is taken from the OVRO observations.